

Development of LTCC Smart Channels for Integrated Chemical, Temperature, and Flow Sensing

Clifford K. Ho, Kenneth A. Peterson, Lucas K. McGrath, and Timothy S. Turner
Sandia National Laboratories
P.O. Box 5800
Albuquerque, NM 87185-0735
Phone: (505) 844-2384; Fax: (505) 844-7354
E-mail: ckho@sandia.gov

Abstract

This paper describes the development of “smart” channels that can be used simultaneously as a fluid channel and as an integrated chemical, temperature, and flow sensor. The uniqueness of this device lies in the fabrication and processing of low-temperature co-fired ceramic (LTCC) materials that act as the common substrate for both the sensors and the channel itself. Devices developed in this study have employed rolled LTCC tubes, but grooves or other channel shapes can be fabricated depending on the application requirements. The chemical transducer is fabricated by depositing a conductive polymer “ink” across a pair of electrodes that acts as a chemical resistor (chemiresistor) within the rolled LTCC tube. Volatile organic compounds passing through the tube are absorbed into the polymers, causing the polymers to reversibly swell and change in electrical resistance. The change in resistance is calibrated to the chemical concentration. Multiple chemiresistors have been integrated into a single smart channel to provide chemical discrimination through the use of different polymers. A heating element is embedded in the rolled tube to maintain a constant temperature in the vicinity of the chemical sensors. Thick-film thermistor lines are printed to monitor the temperature near the chemical sensor and at upstream locations to monitor the incoming ambient flow. The thermistors and heating element are used together as a thermal anemometer to measure the flow rate through the tube. Configurations using both surface-printed and suspended thermistors have been evaluated.

Key Words

LTCC, smart channels, anemometry, thermistor, chemiresistor

1.0 Introduction

Microsensor systems are often comprised of multiple components assembled onto a common platform. The individual components are fabricated separately and later assembled and connected. Assembly of individual sensor components can be complicated, and fluidic interconnects (e.g., for chemical or flow sensors) can occupy significant amounts of space. In this paper, we describe the development of “smart” channels that minimize post-fabrication assembly and interconnects. The smart channel can be simultaneously used as both a fluid channel and an integrated chemical, temperature, and flow sensor.

Low-temperature co-fired ceramic (LTCC) is used as the common substrate for both the channel and sensors. In

contrast, emerging micro-analytical systems have typically utilized individual components fabricated from silicon that are later assembled and mounted onto a common platform with fluidic interconnects [1]. LTCC has several features that make it attractive in the use of integrated sensing and flow, including its ease of fabrication for a variety of shapes such as tubes and channels and its ability to integrate electronic components. A thorough description of LTCC materials and potential applications can be found in [2].

This paper begins with a description of the fabrication of LTCC smart channels. The design and testing of channels in the shape of tubes is presented here, but flat channels are also being investigated [3]. Testing and calibration of the integrated temperature, flow, and chemical sensors are then described in the remaining sections.

2.0 Design and Fabrication of LTCC “Smart” Channels

2.1 Background

Complex LTCC substrates can be fabricated with cavities for many microelectronic multichip module implementations, and these are typically used as boards and devices which are planar. The starting substrates are pliable unfired sheets of glass-ceramic doctor-bladed tapes (DuPont 951AT). Perforations can be made in these tapes for vias and cavities and thick film materials can be screen-printed onto these tapes. These thick films may define circuit features or fill vias for interlayer connectivity. Following the drying of thick films, the tapes are inspected, collated, and laminated together, by a variety of techniques, to form a monolithic structure. Following that, the structure is cofired. Cofiring refers to the simultaneous firing of the substrate, various conductors, and any resistors or other structures that are included in the design. It is also possible to add thick films after cofiring and then refire the part to attain additional functions. Certain non-planar applications have also been enabled by LTCC. These include the rolling of a drift tube for an ion-mobility spectrometer and non-planar microfluidic devices [4].

2.2 Design

The smart channel was designed so that it could be rolled into a tube from a planar LTCC sheet. The internal electrical structures would be accessible from the outside for connectivity after the sheet was rolled. Thermistors, a heater, and chemical sensor (chemiresistor) electrodes were included on one side (the interior) of the sheet, and additional leads were added to the other side (exterior) to provide connectivity with the internal leads (Figure 1).

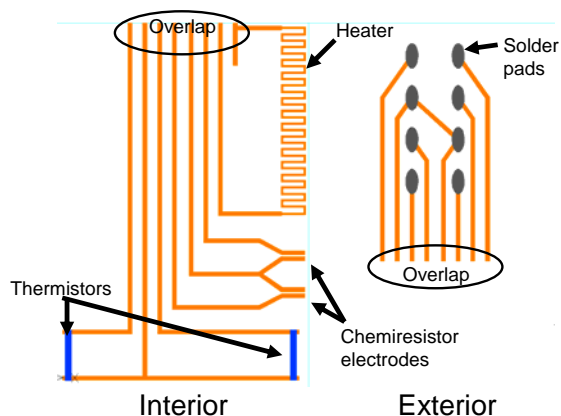


Figure 1. The interior and exterior design layouts combine to provide function and interconnections.

The overlap zone was used to connect the electrical path between thick films on the inner surface (which ends at the overlap) to the thick films on the exterior surface (which begins at the overlap). This overlap is monometallic in this case—both thick films being a pure gold commercial cofirable material (DuPont 5734).

The heater, which is subsequently embedded within the tube during rolling, is used to maintain a constant temperature for the chemiresistor sensor. The leads to the heater were 0.020” in width up to the reduced section, where the serpentine heater consisted of 0.010” wide lines. Chemiresistor electrodes were printed to provide 200 micrometer (0.008”) gaps for the subsequent addition of the transducing polymer material (see Figure 2).

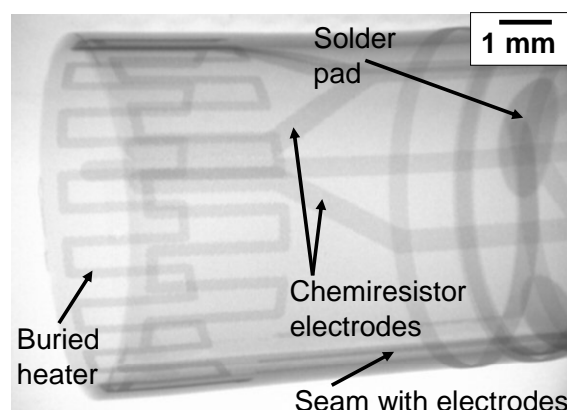


Figure 2. Several integral structures are visible by X-ray.

The chemiresistor electrodes were spaced apart from the heater so that when rolled, they would lie one layer above the embedded heater to allow temperature control. While the thermistors were not vended as a cofirable composition, we have used it several times with good results, as will be shown in a subsequent section.

A thermistor composition (DuPont 5092D, 5093D) was printed near the chemiresistor sensor to monitor the temperature. An upstream thermistor was also included in the design to monitor ambient incoming flows.

The output pads were printed from a cofirable solderable alloy (DuPont 5739) and covered the ends of the output lines from the other structures. They were arranged around the circumference of the middle of the tube. Individual leads were soldered to these pads, formed around the tube, and potted in a molding polymer for durability during testing as shown in Figure 3.

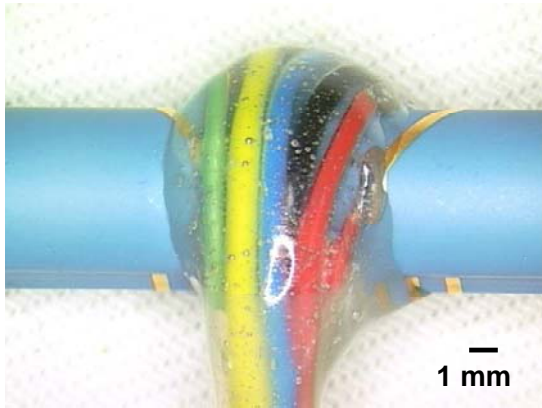


Figure 3. Potted leads increase the handling durability of the tube.

2.3 Fabrication

Having been completely printed, the LTCC tapes were sized in the green state. The leading edge of the substrate was then tapered using an abrasive surface. No thick film structures were placed near the inside seam in this design. The tube was manually rolled on an appropriately-sized smooth metal mandrel. A sufficient number of layers of a polymer film were wrapped around the tube to provide a pad or buffer, permitting us to use a conventional vacuum bagging technique for protection against the aqueous hydraulic fluid in an isostatic laminator. Without the buffer, the bag itself would impress additional undesirable features onto the exterior of the green tube. Following lamination, the buffer was easily removed and the green tube was removed from the mandrel. The tube was fired standing on-end and it supported itself during firing. A powdering inert setter material (Harmonics SPS) was used as a base, and minor deformation which occurred on the lower end was in a cut-off zone. Multiple devices were processed on a single tube and separated after firing.

2.4 Suspended vs. Surface-Printed Thermistors

Elevated structures are useful to a number of different applications. Examples are provided in the literature, including anemometry [5] and a stripline resonator [6]. In the cases cited, the thick film features have been supported on a thin layer of unfired LTCC for cofiring. Thick films may also be applied over a sacrificial material and cofired. During the cofiring cycle, the sacrificial material is removed or is inert and the thick film features that were attached to them are suspended above the substrate with a thermal mass that is very small.

In this study, suspended thermistors were fabricated on a thick film dielectric layer and subsequently separated and

assembled into the tube, using a conductive epoxy as shown in Figure 4. These suspended thermistors were compared to the surface-printed thermistors in the following sections to evaluate the temperature and flow-sensing capabilities. A modification in which the suspended thermistors are completely cofired into place is underway.

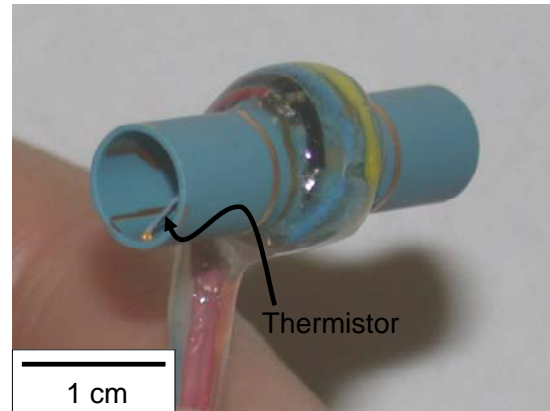


Figure 4. An assembled suspended thermistor is visible near the end of the tube.

2.5 Chemiresistor Fabrication

The chemiresistor sensors are comprised of two electrodes separated by a finite distance. A conductive polymer (“ink”) is deposited over this gap to create an electrical pathway between the two electrodes.

The chemiresistor ink is a mixture of polymer and carbon black dissolved and dispersed in a solvent. Typically the mass of carbon and polymer totals 0.1 g and is mixed in 5 ml of solvent. The solvent is chosen based on the polymers’ solubility. For example, for the polar polymer poly (N-vinyl pyrrolidone) (PNVP), water was used as the solvent. For the other two polymers that were selected for our application, poly(ethylene-vinyl acetate) (PEVA) and poly(isobutylene) (PIB), trichloroethylene (TCE) was used as the solvent.

The polymer/solvent mixture is heated to approximately 40 °C to expedite the dissolution. After the polymer dissolves, a measured quantity of carbon black is added to the mixture. The vials are then placed in a sonicating bath for an hour to increase the dispersion of the carbon in the solution. The ink is then ready to be deposited on the chemiresistor electrodes. For this application three polymer inks, (PNVP, PIB, & PEVA) were created using a 40%/60% carbon black/polymer ratio by weight.

The chemiresistor electrodes on the LTCC surfaces were cleaned with acetone and methanol. A 10 μ L micropipette was used to wick a small amount of ink from the vials. The micropipette was placed directly above the chemiresistor electrodes, and a slight pressure was placed on the top of the

micropipette to push a bead of ink out of the pipette. If a resistance is not measured across the electrodes, more ink can be deposited or the prior deposition can be wiped off with acetone followed by another deposition. Figure 5 shows an image of the polymer ink deposition onto dual chemiresistor electrodes within the rolled LTCC smart channel.

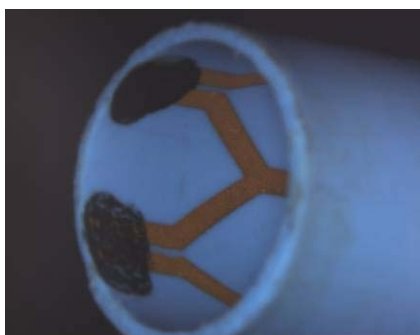


Figure 5. Deposition of polymer inks onto dual chemiresistor electrodes in the LTCC smart channel.

Seven LTCC smart channels were fabricated using different polymer combinations and thermistor configurations (Table 1).

Table 1. Seven LTCC smart-channel devices were fabricated for testing.

Device	Thermistor Configuration	Polymers
110705-1	Suspended	PEVA & PNVP
110705-2	Suspended	PEVA & PNVP
110705-3	Suspended	PEVA & PIB
110705-4	Suspended	PEVA & PIB
072705-4	Surface-printed	PEVA & PIB
072705-5	Surface-printed	PEVA & PIB
072705-7	Surface-printed	PEVA & PNVP

3.0 Calibration and Testing

The LTCC sensors were calibrated to temperature, gas flow, and chemical concentrations. Devices were calibrated to temperature in an oven that was monitored with a T-Type thermocouple. For flow calibrations, flow rates were monitored with an FMA-A208 Mass Flow Meter from Omega. Varying concentrations of different constituents (e.g., water vapor, TCE, m-Xylene) were introduced into the flow stream using bubblers and flow meters. All data were recorded with a CR1000 Campbell Scientific data logger. The CR1000 was also programmed to control the temperature in the vicinity of the chemiresistor sensors using the embedded heater. The temperature of the chemiresistor sensors was maintained at 40 °C by toggling heater power on or off over 60 msec intervals.

For flow and chemical sensing, two LTCC devices were calibrated simultaneously in series. Figure 6 shows a schematic of the test apparatus for the flow and chemical calibrations.

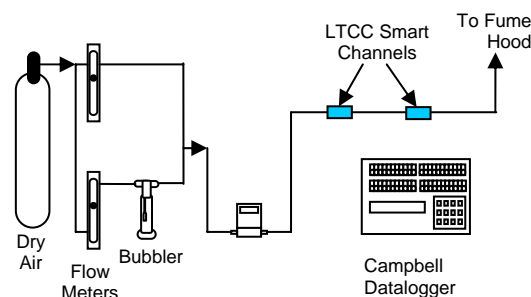


Figure 6. Sketch of the LTCC smart-channel flow and chemical-concentration test apparatus.

The following sections provide additional details regarding the calibration and testing of the temperature, flow, and chemical sensors.

3.1 Temperature Sensing

3.1.1 Calibration Procedure

Two thermistors on each of the LTCC smart channels were calibrated to temperature by placing the devices inside an oven set to 60 °C. The temperature inside the oven was allowed to stabilize before slowly decreasing after the oven was turned off. The resistances of the LTCC thermistors and the oven temperature were recorded using the CR1000. The temperature was plotted as a function of thermistor resistance for each device and a linear regression was applied.

3.1.2 Results

Figure 7 shows the temperature calibrations for four devices, each containing two thermistors. Two devices contained surface-printed thermistors, while the other two devices contained suspended thermistors. All of the thermistor resistances show an excellent linear regression with temperature. The surface-printed thermistor resistances were on the order of several thousand ohms, whereas the suspended thermistor resistances were on the order of several hundred ohms. The corresponding temperature regression for each thermistor (Table 2) was programmed into the CR1000 for additional testing of each device with flow and chemical concentrations.

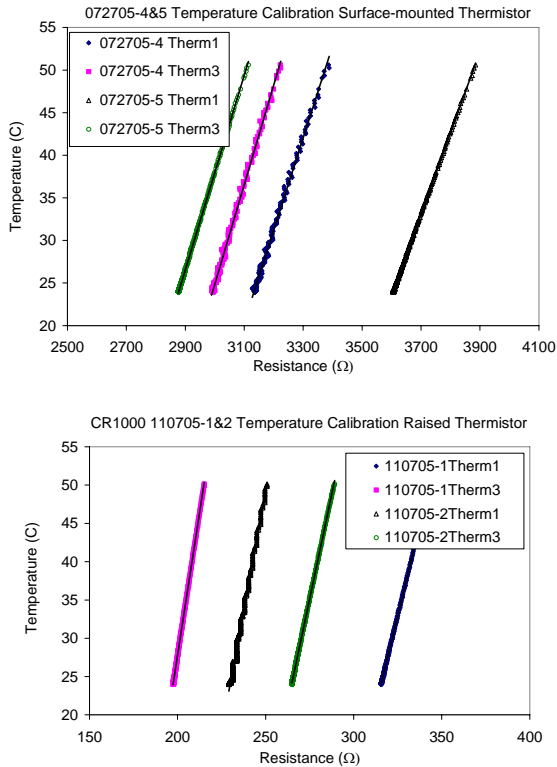


Figure 7. Temperature calibration of surface-printed thermistors (top) and suspended thermistors (bottom).

Table 2. Summary of linear regressions for temperature-calibrated thermistors.

Sensor	Linear Regression	R ²
72705-4Therm1	0.1096x - 319.51	0.9901
72705-4Therm3	0.1164x - 324.35	0.9906
72705-5Therm1	0.0966x - 324.48	0.9983
72705-5Therm3	0.1138x - 303.43	0.9975
72705-7Therm1	0.1345x - 385.23	0.9865
72705-7Therm3	0.1133x - 395.82	0.9925
110705-1Therm1	0.9429x - 273.51	0.9994
110705-1Therm3	1.4974x - 271.85	0.9994
110705-2Therm1	1.1798x - 246.55	0.9877
110705-2Therm3	1.0814x - 262.28	0.9988
110705-3Therm1	0.8761x - 262.42	0.9966
110705-3Therm3	1.4659x - 274.84	0.9989
110705-4Therm1	1.2382x - 281.05	0.9996
110705-4Therm3	1.3121x - 273.31	0.9997

3.2 Flow Sensing (Anemometry)

3.2.1 Calibration Procedure

The LTCC smart channels were calibrated to flow using different gases at various flow rates. The flow rates ranged from 50 mL/min to 600 mL/min in 50 mL/min increments. Sensors were calibrated to each flow rate for 10 minutes. Voltage was applied to the heating element of each device to maintain a constant thermistor temperature of 40 °C (near the heater). The applied voltage was monitored with the CR1000 data logger every 60 msec, and a running average of recorded voltages was taken for a two second period. The average voltage was plotted against the actual flow rate to generate calibration curves. This procedure was repeated for the following gases: dry air, moist air at 100% relative humidity, dry air with 50% TCE, and dry air with 50% m-Xylene.

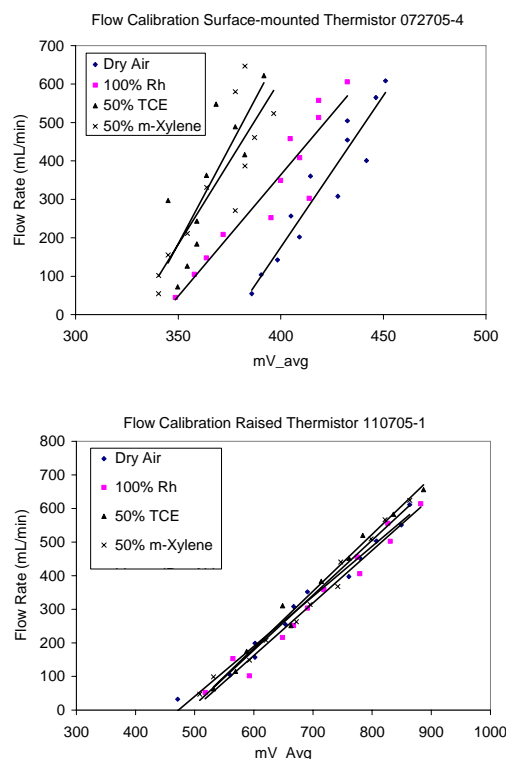
3.2.2 Test Results

Figure 8 shows the flow calibrations for two LTCC smart channels—one device contained surface-printed thermistors, and the other device contained suspended thermistors. The device with surface-printed thermistors yielded more variability in the applied voltage for different gases and flow rates. The suspended thermistors produced much better linear regressions between the applied flow rates and the applied voltage for all the gases tested. We postulate that the suspended thermistors are more sensitive to changes in flow rates since they are within the flow stream. This was also observed in previous studies [5]. The surface-printed thermistors are within a viscous sublayer of flow and are less sensitive to the bulk changes in flow rates. In addition, because the viscosity is different among the different gases used in the calibrations, the flow calibrations for the surface-printed thermistors vary significantly with the different gases.

Therefore, these tests demonstrate that suspended thermistors perform better than surface-printed thermistors for the purposes of anemometry in LTCC smart channels. Table 3 summarizes the flow calibrations for two representative devices exposed to different gas constituents and flow rates. The R² values confirm that the regressions for the suspended thermistors are superior to the regressions for the surface-printed thermistors.

Table 3. Flow calibrations for representative LTCC smart channels with surface-printed thermistors vs. suspended thermistors using different gas constituents and flow rates.

Gas Constituent	Linear Regression			
	Surface-printed Thermistor (072705-4)	R ²	Suspended Thermistor (110705-1)	R ²
Dry Air	$7.8762x - 2974.7$	0.91	$1.4875x - 702.79$	0.98
Moist Air with 100% RH (water vapor)	$6.3221x - 2164.8$	0.89	$1.5658x - 777.45$	0.97
Dry Air with 50% TCE by Volume	$10.032x - 3327.6$	0.67	$1.695x - 832.63$	0.99
Dry Air with 50% m-Xylene by Volume	$8.6134x - 2832$	0.76	$1.6344x - 802.07$	0.98

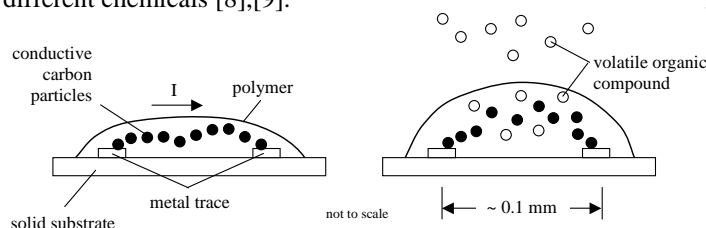
**Figure 8. Flow calibration of surface-printed thermistors (top) and suspended thermistors (bottom).**

3.3 Chemical Sensing

The chemiresistor consists of a chemically-sensitive polymer that is dissolved in a solvent and mixed with conductive carbon particles [7]. The resulting ink is then deposited and dried onto thick-film gold traces printed onto an LTCC tape. When chemical vapors (volatile organic compounds) come into contact with the polymers, the chemicals absorb into the polymers, causing them to swell. The swelling changes the resistance of the electrode, which can be measured and recorded (Figure 9). The amount of swelling corresponds to the concentration of the chemical vapor in contact with the

chemiresistor. The process is reversible if the chemical vapors are removed, but some hysteresis and drift can occur.

The LTCC smart channels evaluated in this paper include two sets of chemiresistor electrodes. Different polymers can be deposited onto each pair of electrodes. By choosing polymers with different affinities to different volatile organic compounds, we can use various chemometric and multivariate regression techniques to discriminate among different chemicals [8],[9].

**Figure 9. Chemiresistor detection of volatile organic compound vapors. Left: Electrical current (I) flows across a conductive thick-film carbon-loaded polymer deposited across a pair of electrodes. Right: Chemicals absorb into the polymer, causing it to swell (reversibly) and break some of the conductive pathways, which increases the electrical resistance. [7]**

3.3.1 Calibration Procedure

Table 1 summarizes the different polymer combinations that were used for each pair of chemiresistor sensors and for each LTCC smart-channel. The PEVA/PNVP polymer combination was used to discriminate solvents such as TCE from water. PEVA has a strong affinity for chlorinated solvents and hydrocarbons, while PNVP has a strong affinity for polar compounds such as water. The PEVA/PIB combination was evaluated for discrimination among TCE and m-Xylene, an aromatic hydrocarbon. Based on these combinations, the chemiresistor sensors were exposed to combinations of either dry air, water vapor, and TCE, or dry air, TCE, and m-Xylene. The concentrations of water vapor that were used included 0%, 50%, and 100% relative humidity (RH). The concentrations of TCE and m-Xylene

that were used included 0%, 50%, and 100% of the constituent's saturated vapor pressure (at 23 °C) in dry air by volume.

The chemiresistor sensors were exposed to chemicals by placing two LTCC smart channels in series with gas flowing at 200 mL/min through each channel. The channels were purged initially for approximately 60 minutes by flowing clean dry air through the lines. During this time the sensors stabilized and a baseline resistance was recorded, R_b . Then the sensors were exposed to a known chemical concentration of water vapor, TCE, or m-Xylene for approximately 60 minutes.

The relative change in resistance for each chemiresistor sensor was used for the calibrations. The equation for the relative change in chemiresistor resistance is as follows:

$$\frac{\Delta R}{R_b} = \frac{R - R_b}{R_b}$$

where R is the measured resistance and R_b is the baseline resistance taken prior to exposure.

3.3.2 Test Results

A typical response of the chemiresistor sensor to chemical exposure is illustrated in Figure 10. The PEVA chemiresistor (device 072705-4) is exposed to dry air and then 25%, 50%, and 100% saturated TCE vapor by volume with dry-air purges in between each exposure. The chemiresistor response is fairly rapid (on the order of seconds), although at such high concentrations, it can take on the order of minutes to reach equilibrium. In Figure 10, it

appears that the PEVA resistances did not reach complete equilibrium before each purge.

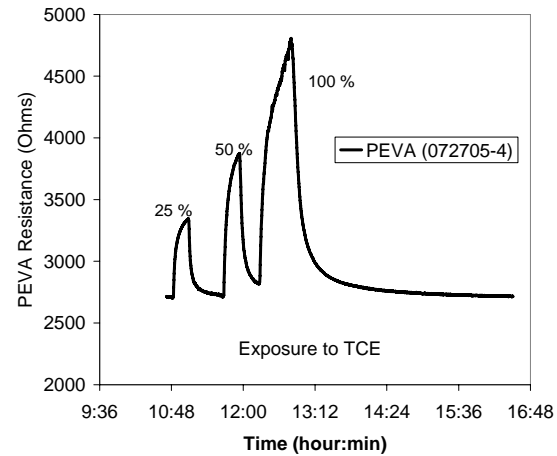


Figure 10. Exposure of PEVA chemiresistor (device 072705-4) to different concentrations of TCE with a clean-air purge in between each exposure.

Figure 11 and Figure 12 show the calibration of two different pairs of chemiresistors to different gas constituents. The PIB/PEVA chemiresistor pair was calibrated to m-Xylene and TCE, and the PNVP/PEVA chemiresistor pair was calibrated to TCE and water vapor (at different relative humidities). Figure 11 shows that the PIB and PEVA polymers are more sensitive to exposure to TCE versus exposure to m-Xylene, but both polymers appear to respond similarly. Therefore, using these two polymers for discrimination of m-Xylene and TCE is not optimal.

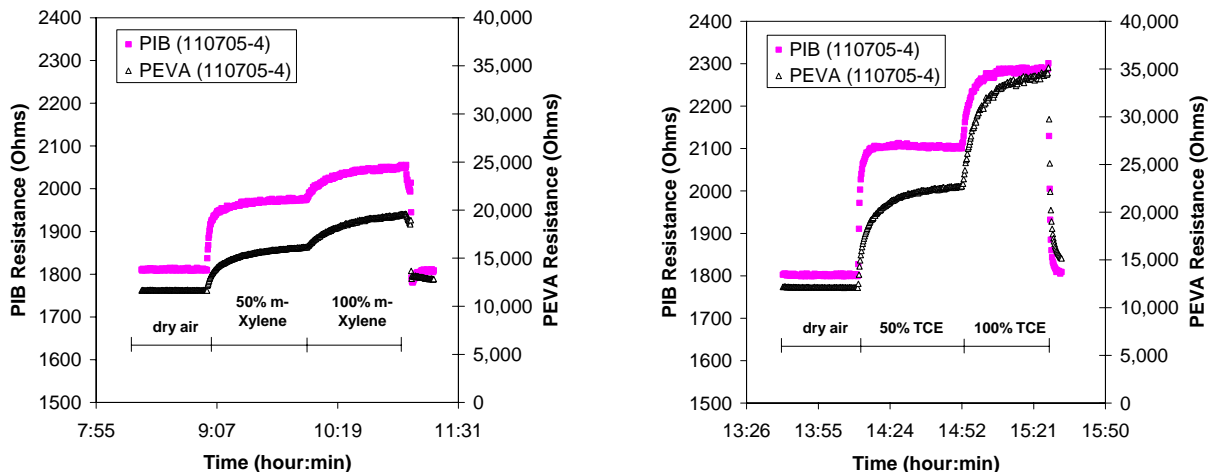


Figure 11. Calibration of PIB/PEVA chemiresistors (on device 110705-4) to m-Xylene (left) and TCE (right).

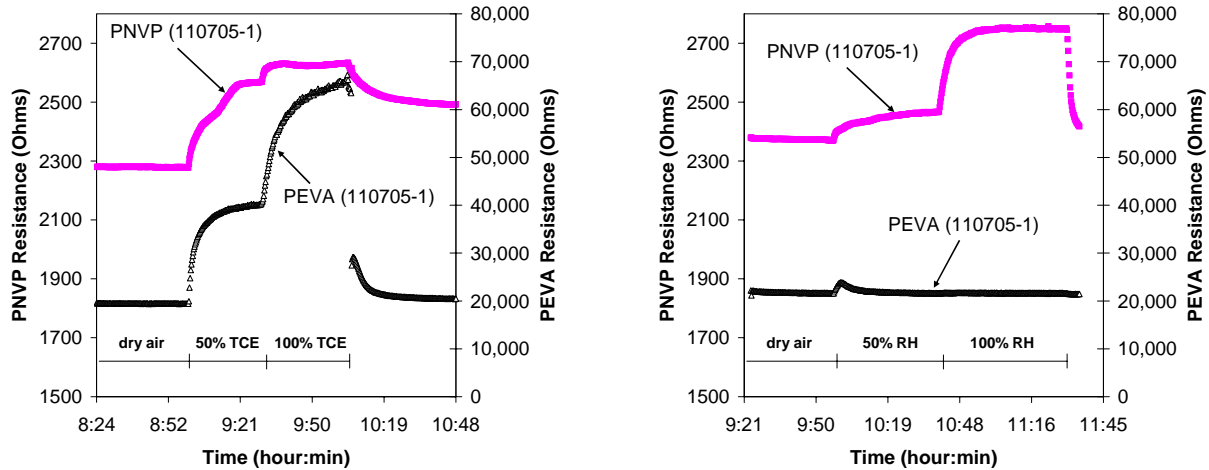


Figure 12. Calibration of PNVP/PEVA chemiresistors (on device 110705-1) to TCE (left) and water vapor (right).

Figure 12 shows that the PEVA polymer has a very strong response to TCE, but very little response to water vapor (the small “blip” in the PEVA response to water vapor at the onset of the 50% relative-humidity exposure was due to the use of a flow line that was previously connected to the TCE bubbler). In contrast, PNVP responds to TCE, but it has a much more stable and definitive response to water vapor. Therefore, the use of the combined PNVP and PEVA chemiresistors should allow reasonable discrimination between TCE and water vapor.

The results of the PNVP/PEVA calibrations (for device 110705-1) were used to develop multivariate polynomial regressions to estimate the TCE and water-vapor concentrations as a function of the relative change in resistances for both PNVP and PEVA. The commercial statistical software package Statistica® was used to generate multivariate regressions with a forward stepwise regression analysis to calculate relative-humidity and TCE concentrations:

Relative Humidity:

$$RH(\%) = -0.163 + 1450 \left(\frac{\Delta R}{R_b} \right)_{PNVP} - 5130 \left(\frac{\Delta R}{R_b} \right)_{PNVP}^2 - 137 \left(\frac{\Delta R}{R_b} \right)_{PEVA} + 39.4 \left(\frac{\Delta R}{R_b} \right)_{PEVA}^2$$

TCE (% saturated vapor):

$$TCE(\%) = 0.584 + 42.2 \left(\frac{\Delta R}{R_b} \right)_{PEVA}$$

Results showed that the relative humidity was a function of both PNVP and PEVA, but the TCE concentration was a function of PEVA only. Because the PEVA responded significantly to TCE (and minimally to water vapor), the

forward stepwise regression analysis found that the TCE concentration could be calculated using PEVA alone. However, because PNVP responded to both water vapor and TCE, additional terms were needed to calculate the relative humidity to compensate the response of PNVP to TCE. The coefficient of determination (R^2) for both regressions is greater than 0.99.

The effectiveness of these regressions was tested by exposing the LTCC smart channel (110705-1) to both water vapor and TCE in successive exposures with dry-air purges in between. Figure 13 shows the actual and predicted concentrations as a function of time.

The regression for water vapor concentration (relative humidity) does a good job in predicting the prescribed relative humidity values during the experiment, but there are some erroneous jumps in the predicted relative humidity during the exposure to TCE (Figure 13). The regression for relative humidity was based on steady values of resistances achieved when the chemiresistors had reached equilibrium during the calibrations. Therefore, sharp changes in the resistances of PEVA when the TCE is turned on or off can erroneously affect the predicted relative humidity since the resistance values were not in equilibrium.

The predicted TCE concentration (% saturation) is quite good throughout the entire experiment. The regression correctly predicts a TCE concentration near zero when the chemiresistors are exposed only to water vapor, and the regression predicts fairly accurate values of TCE concentration during the TCE exposures. The predicted TCE concentration at an exposure of 100% saturated TCE vapor is about 10% larger than the actual value.

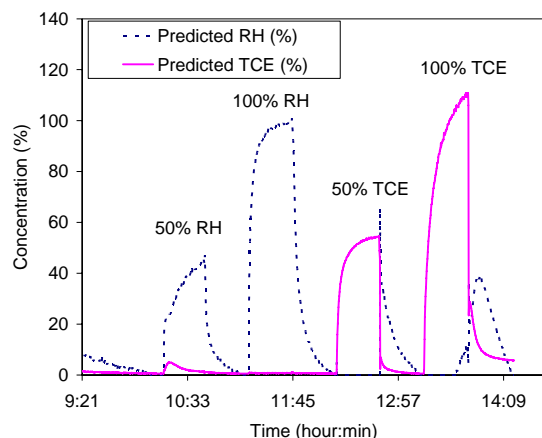


Figure 13. Predicted concentrations of water vapor (% relative humidity, RH) and saturated TCE vapor (%) as a function of time during successive exposures with dry-air purges in between. Actual concentrations are shown as labels above each peak.

4.0 Summary and Conclusions

Smart channels consisting of temperature, flow, and chemical sensors have been fabricated from LTCC. Tubular channels have been investigated in this paper, but flat channels are also being evaluated. Thick-film thermistors were integrated into the channels as temperature sensors, and a heating element was used in conjunction with the thermistors to provide anemometry. Both surface-printed and suspended thermistors were fabricated and evaluated.

Results showed that all of the thermistor resistances yielded linear responses to changes in temperature. However, the suspended thermistors were superior to the surface-printed thermistors in providing linear regressions of flow rate as a function of power (voltage) added to the heater for different gases.

Chemiresistor sensors were integrated into the LTCC channels to provide quantitative detection of volatile organic compounds. Pairs of chemiresistors were included in each channel to evaluate discrimination capabilities among different chemicals. Results showed that the PNVP/PEVA polymer combination yielded reasonable quantitative predictions of water-vapor and TCE concentrations using multivariate regressions.

Future work will focus on improving the design of the suspended thermistors to refine a single-step fabrication process. Flat LTCC smart channels will also be developed for integration with other devices and applications in planar configurations.

Acknowledgments

The authors would like to thank Dennis De Smet for his technical assistance. Sandia is a multiprogram laboratory operated by Sandia Corporation, a Lockheed Martin Company for the United States Department of Energy's National Nuclear Security Administration under contract DE-AC04-94AL85000.

References

- [1] R.P. Manginell, P.R. Lewis, D.R. Adkins, R.J. Kottenstette, D. Wheeler, S. Sokolowski, D. Trudell, J. Byrnes, M. Okandan, J.M. Bauer, and R.G. Manley, "Recent Advancements in the Gas-Phase MicroChemLab,™" in Proceedings of SPIE Vol. 5591, edited by L.A. Smith and D. Sobek, Bellingham, WA, December 2004.
- [2] M.R. Gongora-Rubio, P. Espinoza-Vallejos, L. Sola-Laguna, and J.J. Santiago-Aviles, "Overview of Low Temperature Co-Fired Ceramics Tape Technology for Meso-System Technology," *Sensor. Actuat. A*, 89 222–241, 2001.
- [3] K.A. Peterson, K.D. Patel, C.K. Ho, S.B. Rohde, C.D. Nordquist, C.A. Walker, B.D. Wroblewski, and M. Okandan, "Novel Microsystem Applications with New Techniques in Low-Temperature Co-Fired Ceramics," *Int. Journal of Applied Ceramic Technology*, 2 (5) 371–389, 2005.
- [4] K. A. Peterson, S.B. Rohde, K.B. Pfeifer, T.S. Turner, "Novel LTCC fabrication techniques applied to a rolled ion mobility spectrometer," *Electrochem. Soc. Series*, 27, 156-171, October 2003.
- [5] M. Gongora-Rubio, L.M. Sola-Laguna, P.J. Moffett, J.J. Santiago-Aviles, "The utilization of low temperature co-fired ceramics (LTCC-ML) technology for meso-scale EMS, a simple thermistor based flow sensor," *Sensors and Actuators A*, v73, no3, 215-221, 1999.
- [6] Y.C. Lee and C.S. Park, "A Novel High-Q Stripline Resonator for Millimeter-Wave Applications," *IEEE Microwave and Wireless Components Letters*, V13, No.12, 499-501, 2003.
- [7] C.K. Ho and R.C. Hughes, 2002, "In-Situ Chemiresistor Sensor Package for Real-Time Detection of Volatile Organic Compounds in Soil and Groundwater," *Sensors*, 2, 23-34, 2002.
- [8] T.P., Vaid, T.P., M.C. Burl, and N.S. Lewis, "Comparison of the performance of different discriminant algorithms in analyte discrimination tasks using an array of carbon black-polymer composite vapor detectors," *Analytical Chemistry*, 73(2), 321-331, 2001.
- [9] J.W. Grate and B.M. Wise, "A method for chemometric classification of unknown vapors from the responses of an array of volume-transducing sensors," *Analytical Chemistry*, 73(10), 2239-2244, 2001.